The Neper/FEPX Framework and its Application to the Study of Intra-grain Orientation Distributions in Deformed Aluminium

Romain Quey[1], Loïc Renversade[1] and Matthew Kasemer[2]

New Opportunities in Diffraction Microscopy Workshop, ESRF, Grenoble, 08–11 January 2024

[1] CNRS, MINES Saint-Étienne, France
[2] University of Alabama, USA

Scientific Context: Polycrystal Plasticity Studies by Experiment and Simulation, involving Grain Tracking

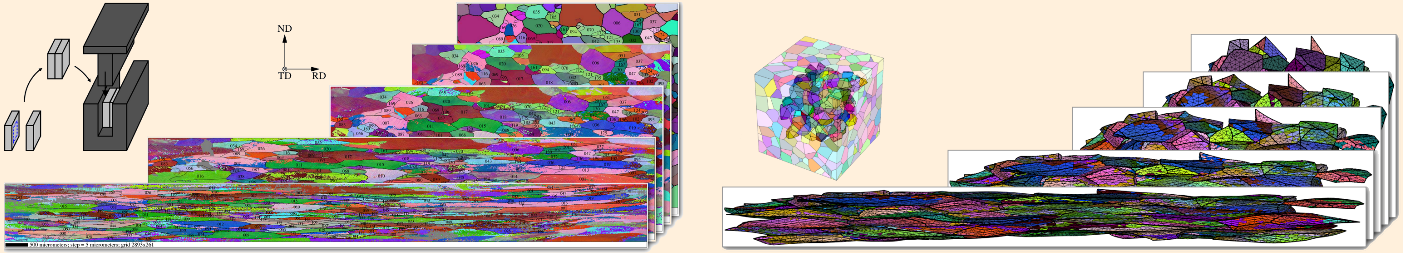

Microtexture tracking (Quey, Dawson and Driver, 2010–2015)

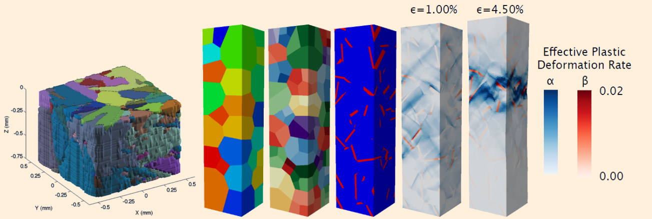

Deformation of Ti64 (Kasemer, Quey and Dawson, 2017)

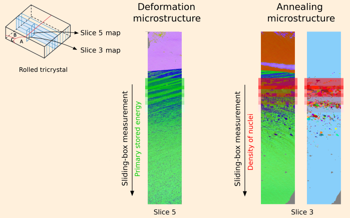

Recrystallization Nucleation in Al (Quey et al, 2022)

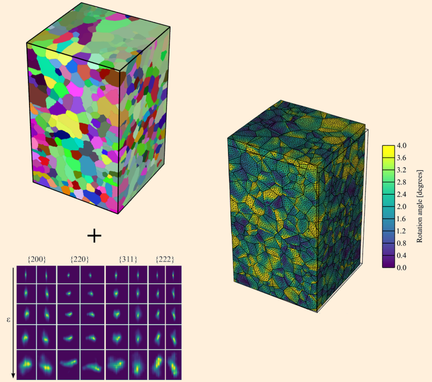

Orientation distributions in Al (Quey et al, 2024)

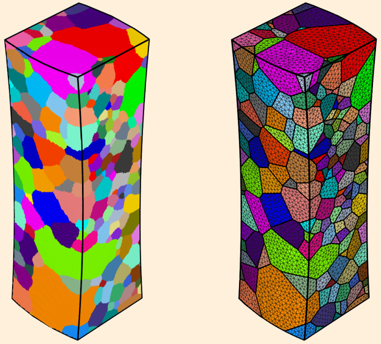

Orientation fields in Al (in progress)

1a/ Experiment 1b/ Simulation 2/ Post-processing 3/ Analysis

Neper/FEPX

Outline

The Neper/FEPX Framework

Intra-grain Orientation Distributions in Deformed Aluminium (Acta Materialia, 2024)

Outline

The Neper/FEPX Framework

Intra-grain Orientation Distributions in Deformed Aluminium (Acta Materialia, 2024)

Neper/FEPX History

	90s–2000s	late 2000s	2010–2011	2011–2019	2020–2023
Neper	Microstructure modelling, phase transformation *Transformation-induced plasticity (Barbe et al, 2008)* 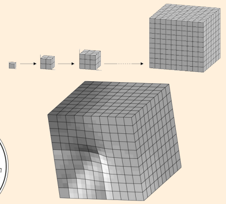	HR random polycrystals, robust meshing *Deformation bands (Barbe et al, 2008)* 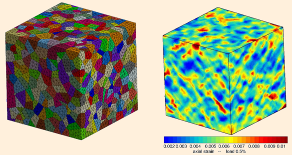 2009: First Neper release	Large deformations, remeshing, Neper & FEPX coupling *Microtextures (Quey et al, 2010–15)* 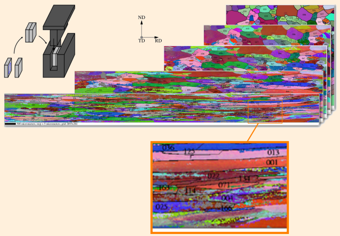 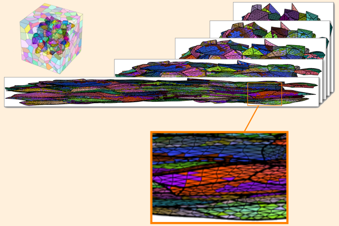	Experimental or complex microstructures *Grain rotations (Renversade and Quey, 2024)* 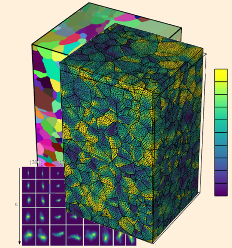	Complete workflow (experiment / simulation) *Neper/FEPX project (Quey and Kasemer, 2022)* 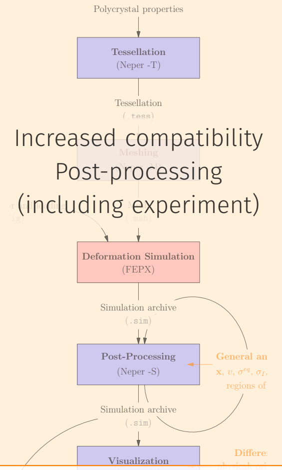 Increased compatibility Post-processing (including experiment)
FEPX	CPFEM, parallel implementation *Sheet forming (Beaudoin, Dawson et al, 1995)* 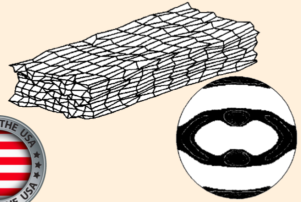	HR (regular) polycrystals *Lattice strains (Wong et al, 2009, vs Bernier @ CHESS)* 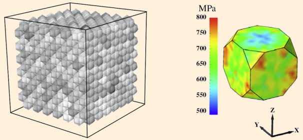		*Deformation of Ti64 (Kasemer et al, 2017)* 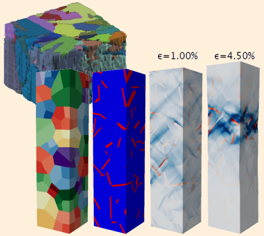	2022: First FEPX release 2024: FEPX v2, implementation @ CHESS
	Macroscopic properties	*Localization, statistical (grain populations)*	*Localization, statistical, intragranular*	*Localization, individual grains, intragranular*	*Workflow standardization*

4 Colleges

1. Publications
2. Data
3. Software → Open-Source Software Award (2021, 2023): Scientific / Documentation / Community
4. Practices

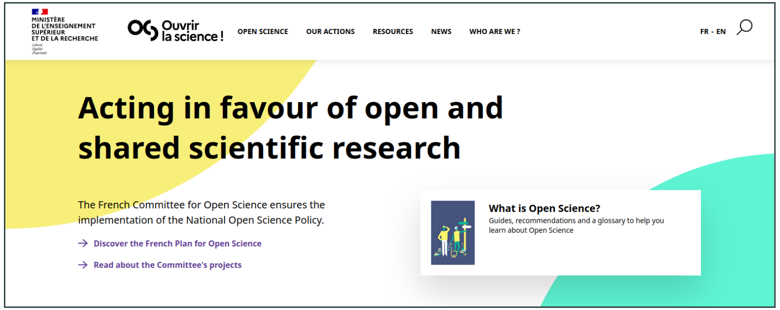

Focus on the French Plan for Open Science

4 Colleges

1. Publications
2. Data
3. Software → Open-Source Software Award (2021, 2023): Scientific / Documentation / Community
4. Practices

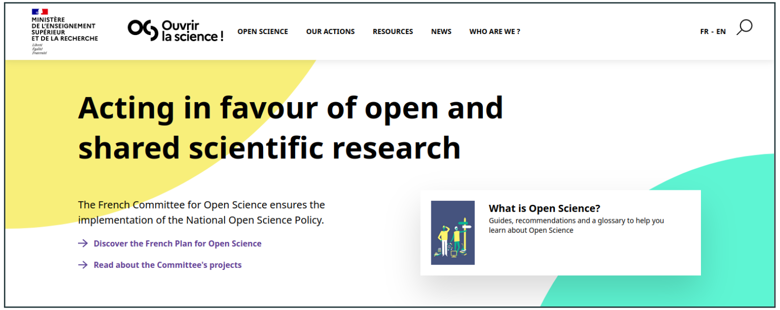

	Crashing Code on GitHub (!)	Neper 2020	Neper 2024
Diffusion	✓	✓	✓
Open-source license	✗	✓	✓
SaaS mode	✗	✗	✗
Published	✗	✗	✓
Used in research	✗	✓	✓
Used in other projects	✗	✗	✗
Cited in publications	✗	✓	✓
Publication list	✗	✓	✓
Forge used	✓	✓	✓
Development workflow	✗	✗	✓
Tests	✗	✗	✓
Code versioning	✓	✓	✓
Bug tracking	✗	✓	✓
Package	✗	✗	✗
Documentation generation	✗	✗	✗
Stable vs devel branch	✗	✓	✓
Continuous integration	✗	✓	✓
Reference manual	✗	✓	✓
Example data	✗	✗	✗
On-line demos	✗	✓	✓
Multilingual documentation	✗	✗	✗
Developers' documentation	✗	✗	✓
Tasks for new developers	✗	✗	✓
Worldwide use	✗	✓	✓
Standard software	✗	✓	✓
Society impact	✗	✗	✗
Used by companies	✗	✓	✓
Users' workshop, forum, blog, chat…	✗	✓	✓
Developers' conferences, management…	✗	✗	✗
Decision making	✗	✗	✗
External modules	✗	✓	✓

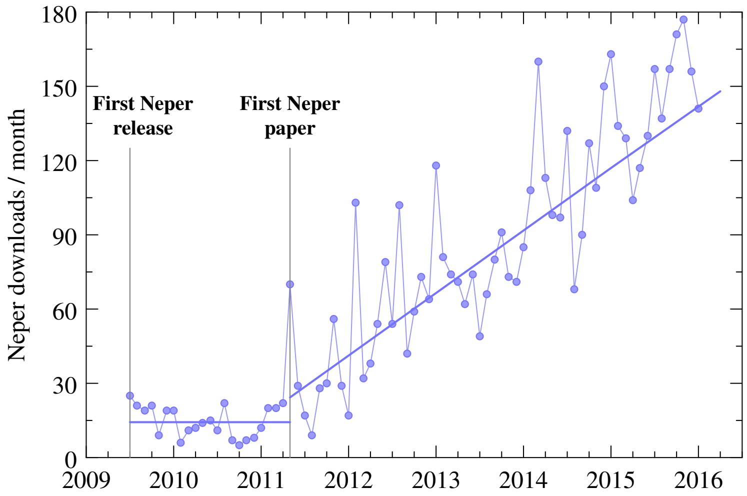

Publishing is very important for a software

Neper/FEPX Overview

https://neper.info

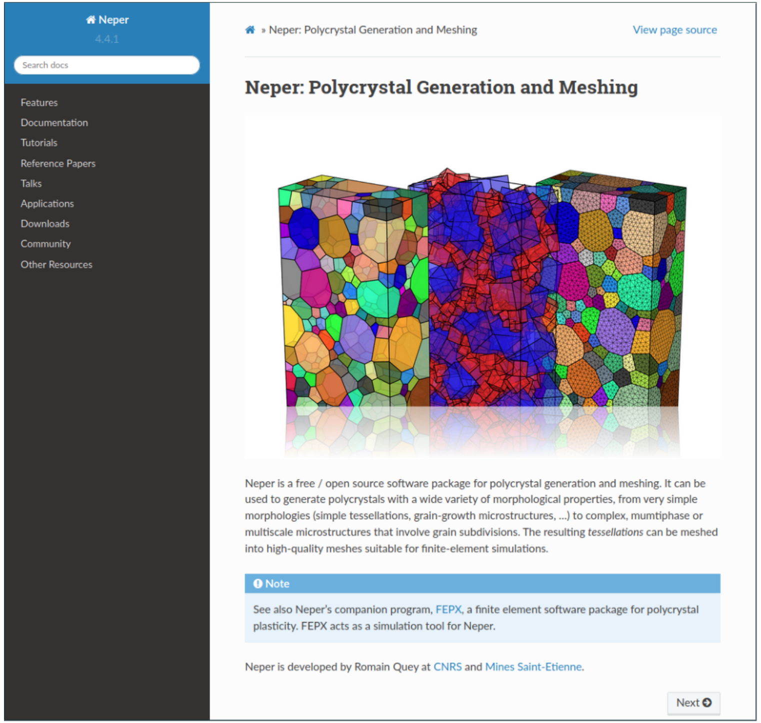

https://fepx.info

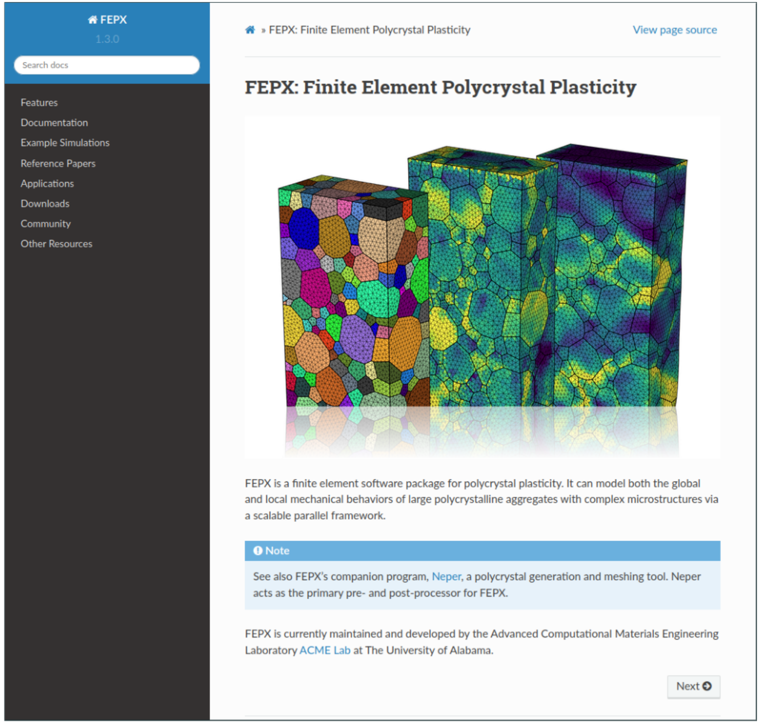

Wide array of resources

Hosted on GitHub (source code, forum, etc.)

Run on personal computer (Neper) / cluster (FEPX)

Easy to install

Simulation (from Experiment)

Experiment

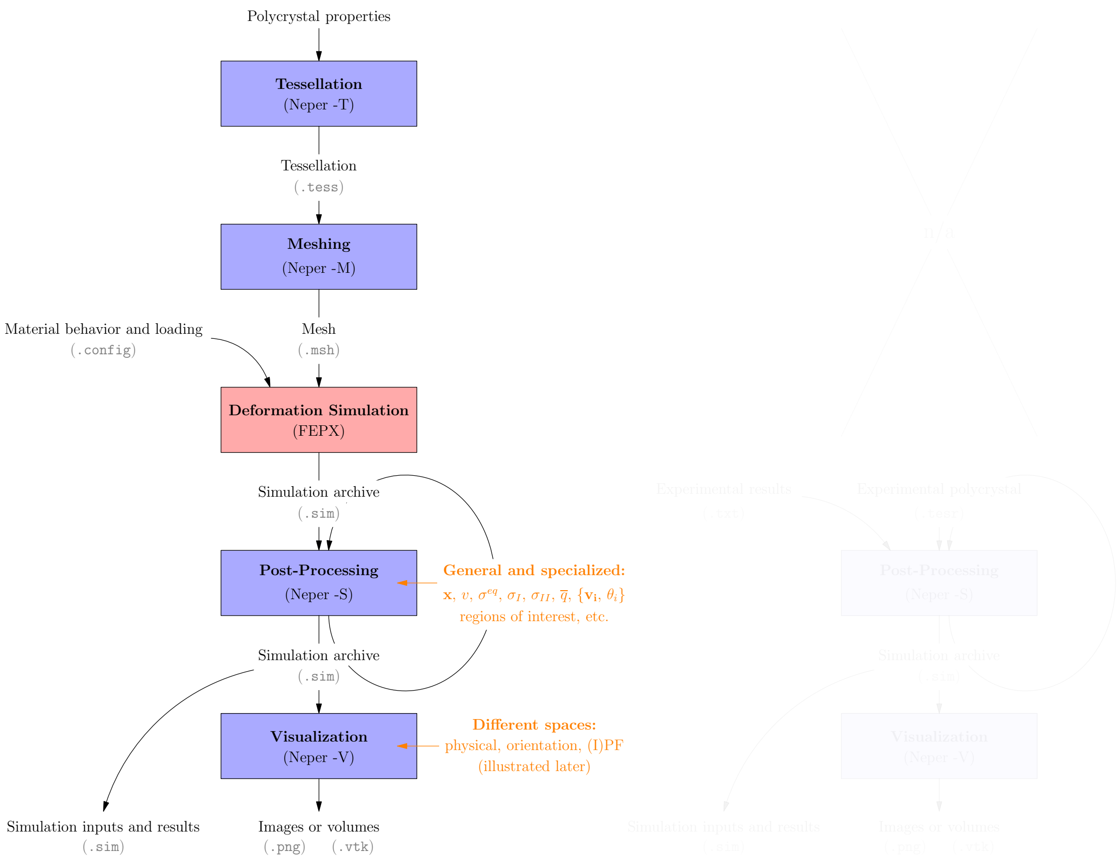

Neper modules / FEPX to run successively

Standalone "concept" file formats

- `tess`: Tessellation/polycrystal file (full info.)
- `tesr`: Experimental polycrystal file (full info.)
- `msh`: Mesh file (full info.)
- `config`: Material + loading file
- `sim`: Simulation database

→ fits different needs

Neper/FEPX Workflow

Simulation (from Experiment) | Experiment

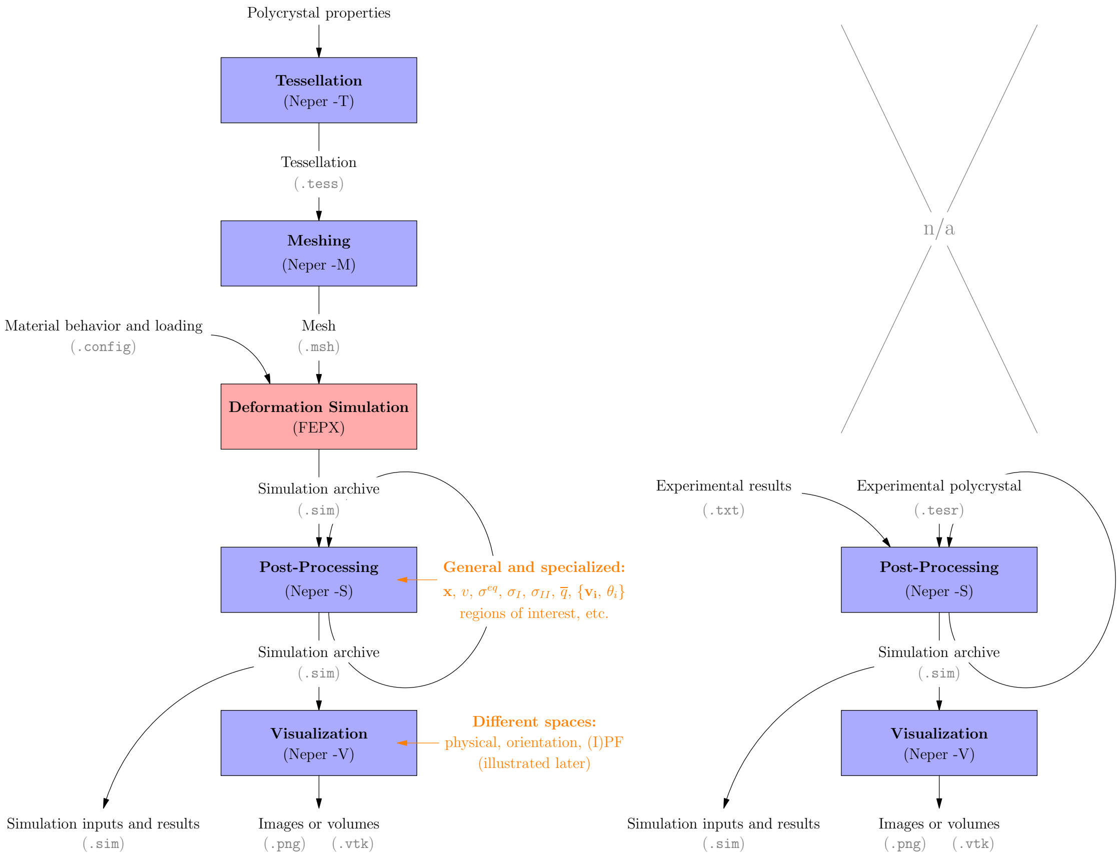

Neper modules / FEPX to run successively

Standalone "concept" file formats

- `tess`: Tessellation/polycrystal file (full info.)
- `tesr`: Experimental polycrystal file (full info.)
- `msh`: Mesh file (full info.)
- `config`: Material + loading file
- `sim`: Simulation database

→ fits different needs

Single-Scale Microstructures

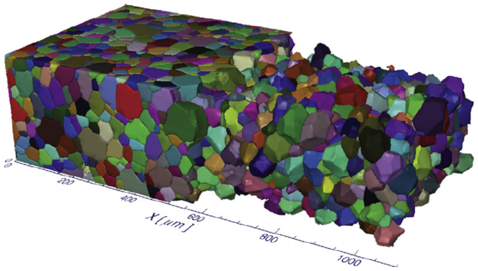

(Rowenhorst et al., 2010)

Multiscale Microstructures

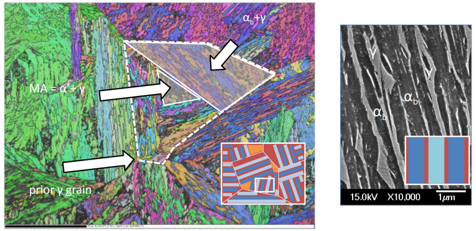

Carbide-free bainitic steel (Hell, 2011)

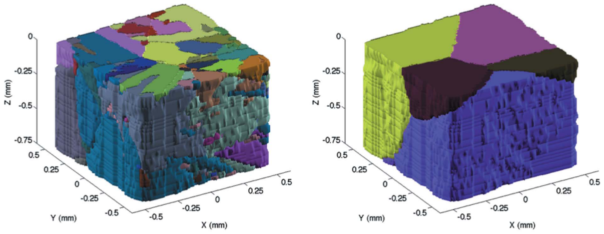

Lamellar Ti64 & parent β grains (Wielewski et al., 2015)

⇝ Single-scale and multiscale have different topologies

Different Types of Experimental Inputs

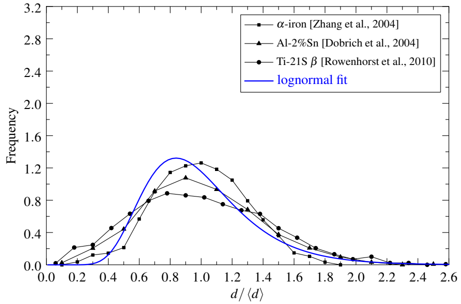

Statistical Data

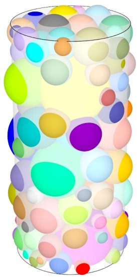

Incomplete Grain Data (3DXRD)

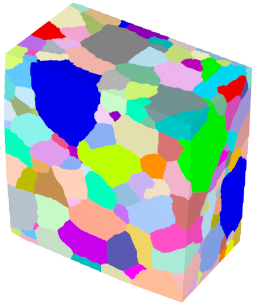

Grain Maps (DCT)

Objective: one general method for all microstructures and inputs

Note: Vectorial Geometry

Definition (E. Laguerre, 1834–1886)

- Domain of space, D
- N seeds, S_i, of positions $\boldsymbol{x}_i$ and weights w_i
- $C_i = \{P(\boldsymbol{x}) \in D \mid d(P, S_i) < d(P, S_j) \ \ \forall j \neq i\}$

$$d\,(P, S_i) = d_E\,(P, S_i)^2 - w_i \quad (\text{"Power distance"})$$

In general, the larger the weight, the bigger the cell.
The weight is equivalent to a sphere radius: $w_i = {r_i}^2$.

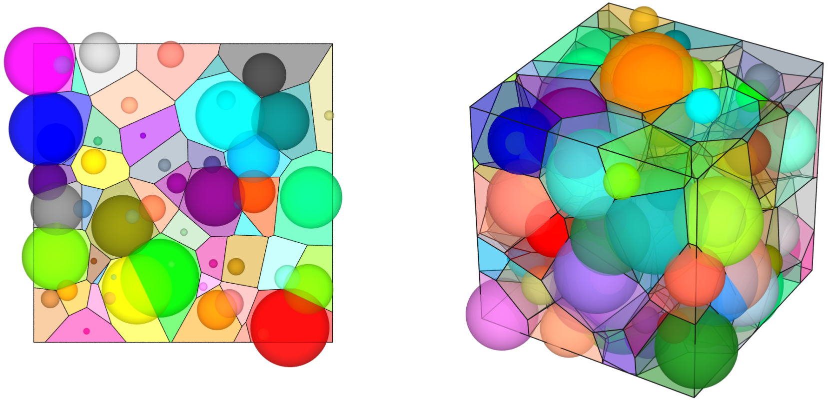

Common Use: Dense Sphere Packing

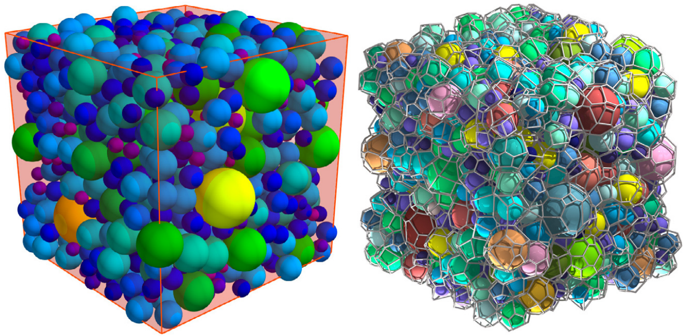

(Chen and Zhao, 2022) for a powder

However, Laguerre Tessellations are General (Lautensack, 2007)

Every normal tessellation of $\mathbb{R}^3$ is a Laguerre tessellation

$\Downarrow$

Laguerre tessellations

=

general parameterization of (convex-grain) polycrystals

(N grains require $4\,N$ uncorrelated parameters)

Optimization Problem

- Variables: for each seed, 3 coordinates + 1 weight ($4 \times N$)
- Objective function: application dependent (grain size distributions, grain centroids, ...)
- Nature: Non-linear, unknown gradient, large-scale, local

Resolution

- Optimization algorithm from the literature (Subplex, from NLopt)
- Tessellation algorithm: cell-based, with update

General optimization

⇓

Retained Laguerre tessellation generality

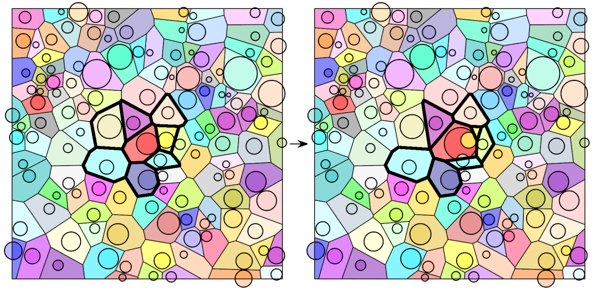

Red seed modified

Any (convex-grain) polycrystal can be generated given proper definition of the objective function

Microstructure Properties

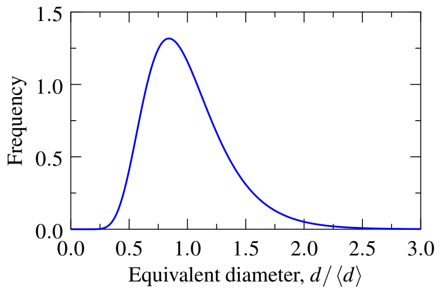

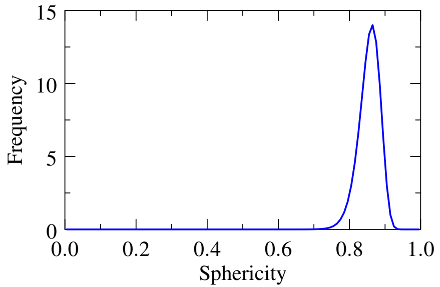

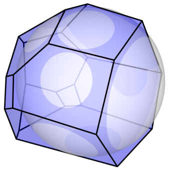

Initial Solution: Voronoi Tessellation

$\mathbf{x}_i$: random
w_i: constant = $\langle r\rangle^2$

Objective Function

Adaptation of the Anderson-Darling test (1952)

For each variable:

$$O = \int_{-\infty}^{+\infty} \frac{(F_S^*(x) - F_S(x))^2}{F_S(x)\,(1 - F_S(x))}\,\mathrm{d}x$$

$F_S^{(*)}(x) = F^{(*)} \circ S$, S: normal distribution

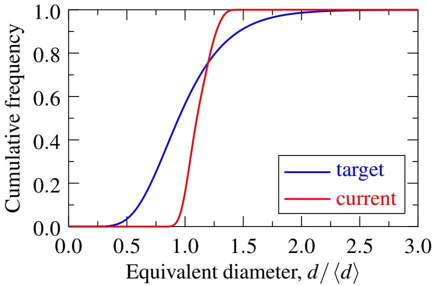

All variables $O = \sqrt{{O_{size}}^2 + {O_{sphericity}}^2}$

Microstructure

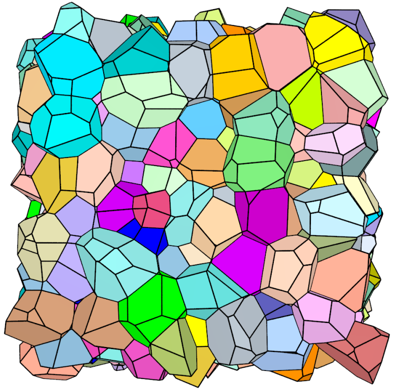

Microstructure Properties

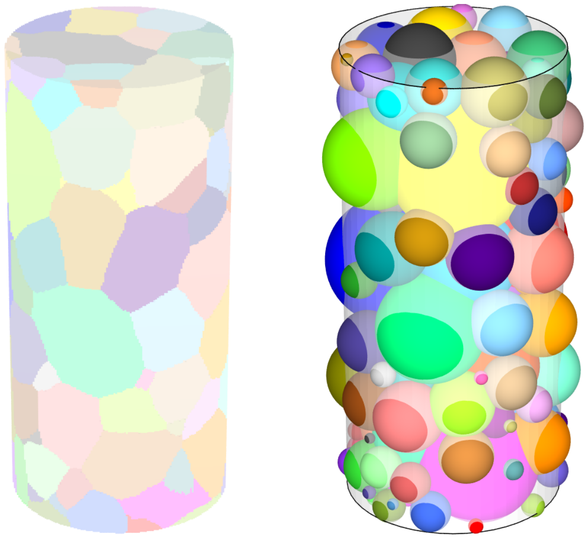

DCT data → ff-3DXRD data

Grain centroids and volumes → spheres

(courtesy H. Proudhon)

Initial Solution

x_i = grain centroid

w_i = (grain radius)^2

Objective Function

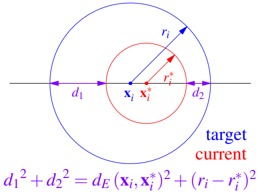

$$\mathcal{O} = \frac{1}{N \langle d \rangle} \sum_i (d_1{}^2 + d_2{}^2)$$

Microstructure

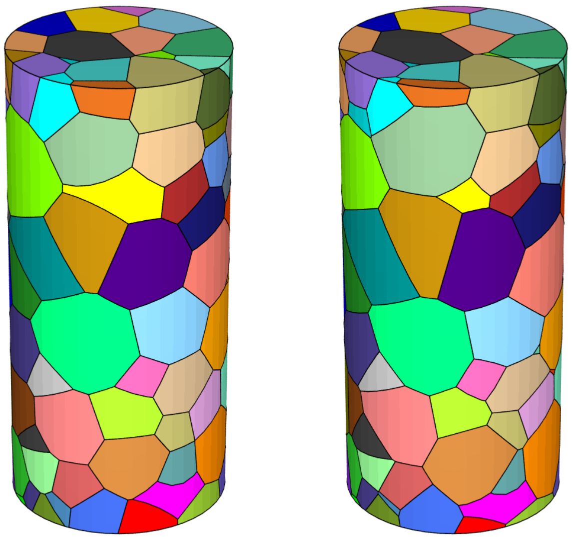

Initial solution: $\mathcal{O} = 0.0149$

Final solution: $\mathcal{O} = 0.00263$

Microstructure Properties

DCT polycrystal

(courtesy H. Proudhon)

Initial Solution

x_i = grain centroid

w_i = (grain radius)^2

Objective Function

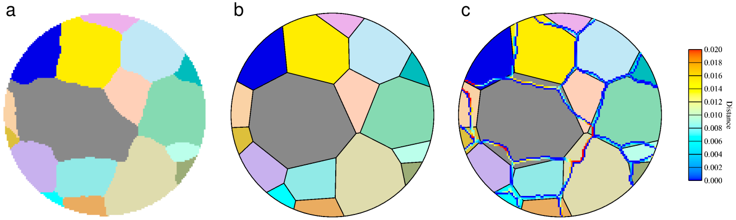

polycrystal tessellation distance

$$\mathcal{O} = \frac{2}{n_v \langle d \rangle} \sum_{i=1}^{N} \sum_{v_k \in G_i^b} d_E(v_k, C_i)^2$$

Microstructure

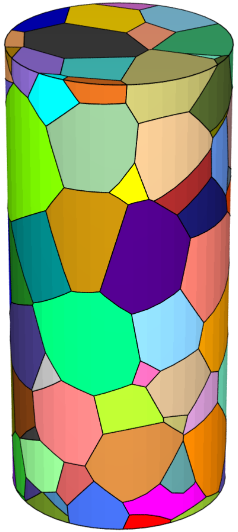

Final solution:

5.6% difference

Particularly interesting for 1/ convex grains (or approximation acceptable), 2/ large polycrystals and 3/ noisy data

Multiscale Microstructures using Nested (Laguerre) Tessellations

Principle: Replicating Material's Processing (Example of Bainitic Steel)

- Scale 1: grain-growth statistics, random orientations
- Scale 2, in each cell:
  - Morphology: seeds on GBs + Voronoi tessellation
  - Orientations: KS, NW relationships, …
- Scale 3, in each cell: lamellae

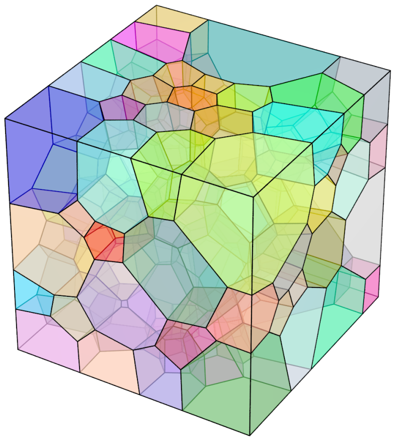

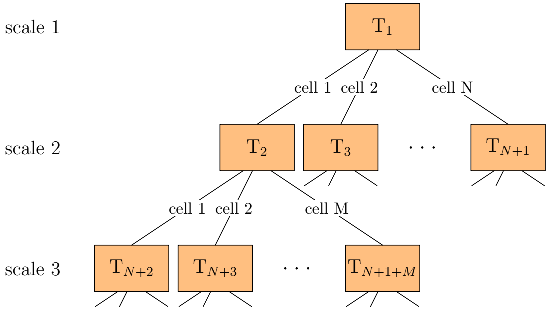

Before Meshing: Flattening

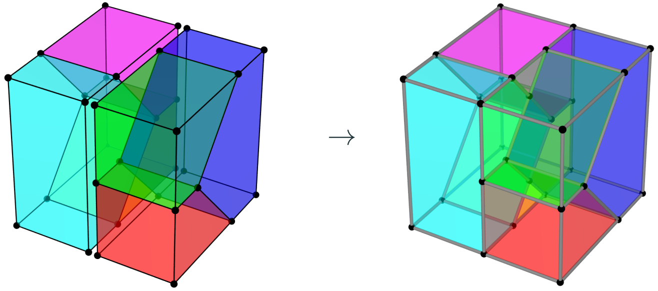

Flattening of a 2-scale tessellation

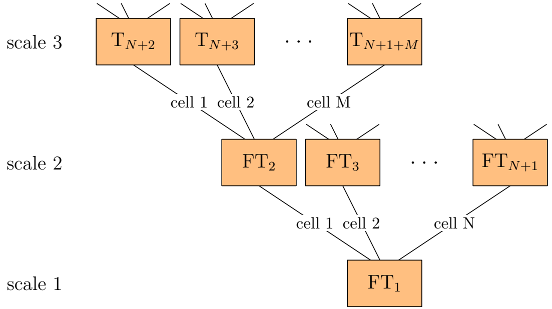

Principle: Replicating Material's Processing (Example of Bainitic Steel)

- Scale 1: grain-growth statistics, random orientations
- Scale 2, in each cell:
  - Morphology: seeds on GBs + Voronoi tessellation
  - Orientations: KS, NW relationships, ...
- Scale 3, in each cell: lamellae

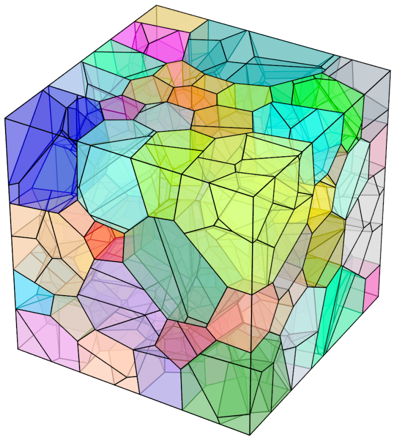

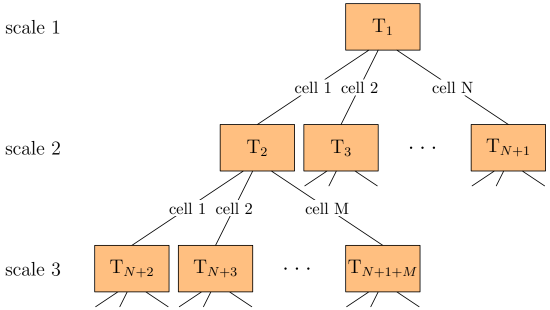

Before Meshing: Flattening

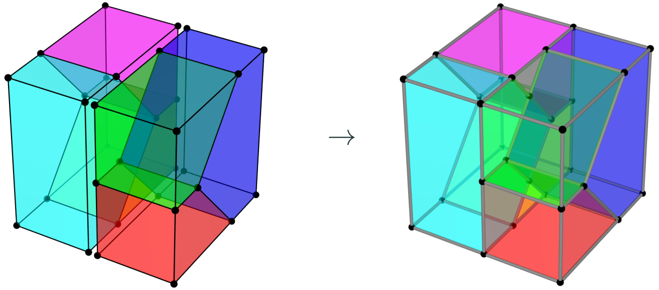

Flattening of a 2-scale tessellation

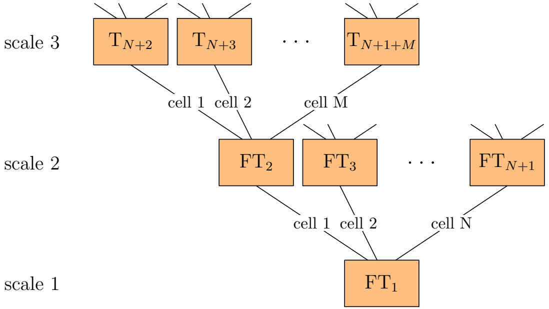

Principle: Replicating Material's Processing (Example of Bainitic Steel)

- Scale 1: grain-growth statistics, random orientations
- Scale 2, in each cell:
  - Morphology: seeds on GBs + Voronoi tessellation
  - Orientations: KS, NW relationships, ...
- Scale 3, in each cell: lamellae

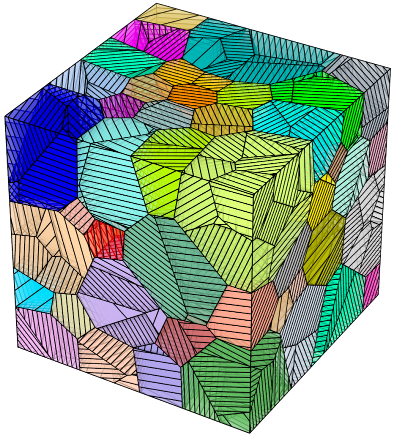

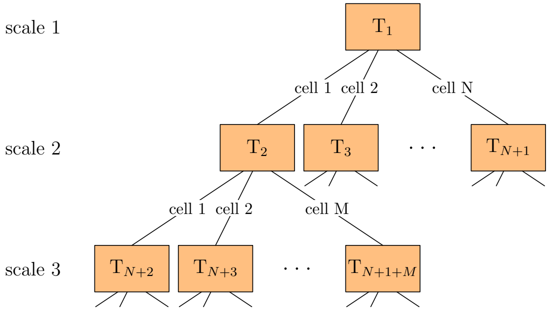

Before Meshing: Flattening

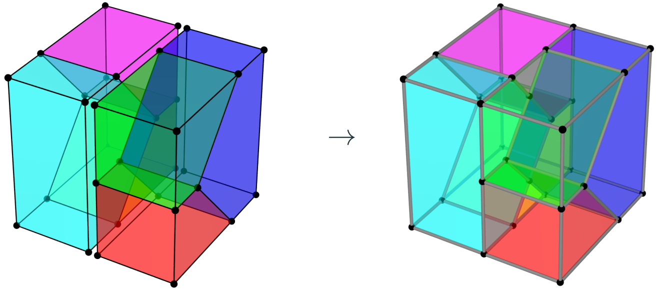

Flattening of a 2-scale tessellation

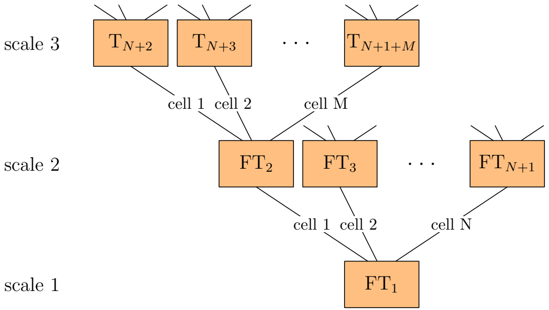

Examples of Multiscale Tessellations

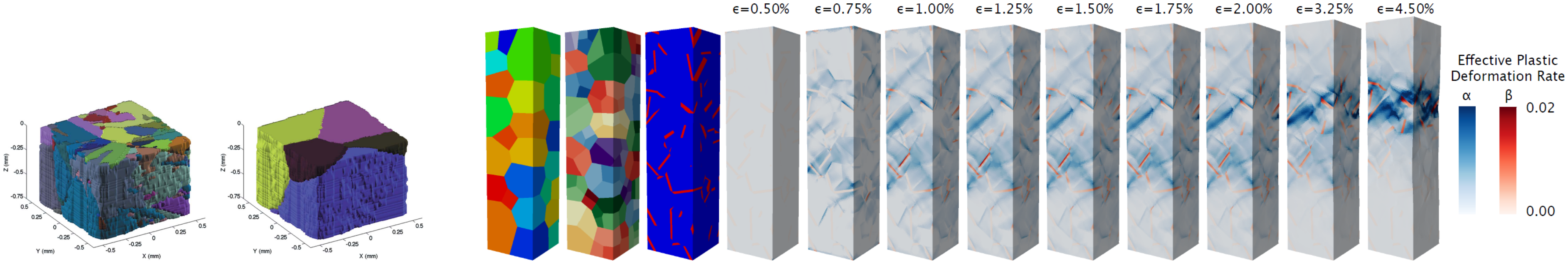

Deformation of Ti64 (Kasemer et al, 2017)

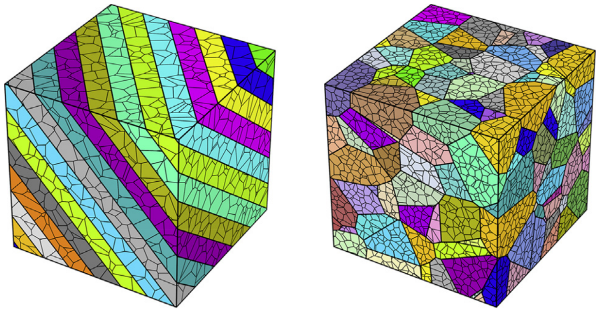

(Left) Sedimentary rocks, (right) intra-grain cracking path (Ghazvinian et al, 2014)

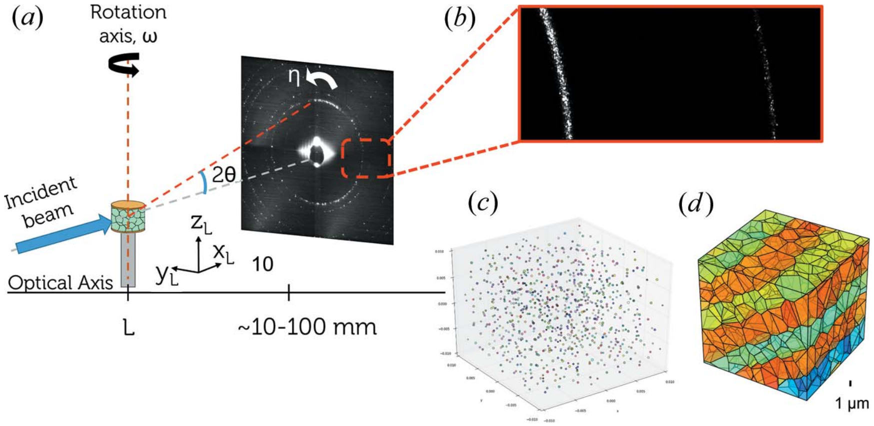

Subgrain structures (Kutsal, Poulsen et al, 2022), ID03

Regularization: $\varepsilon = 1\text{–}3\% \rightarrow \varepsilon = 30\text{–}40\%$

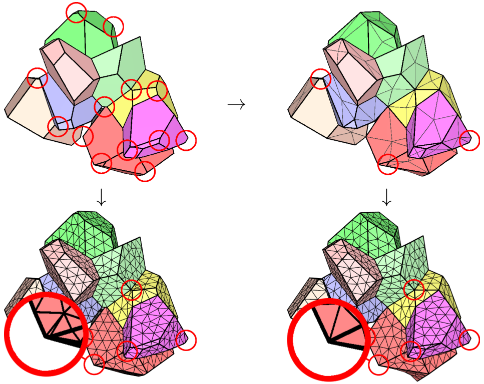

Multimeshing: $N \simeq 1000$ grains $\rightarrow N = 100{,}000$ grains

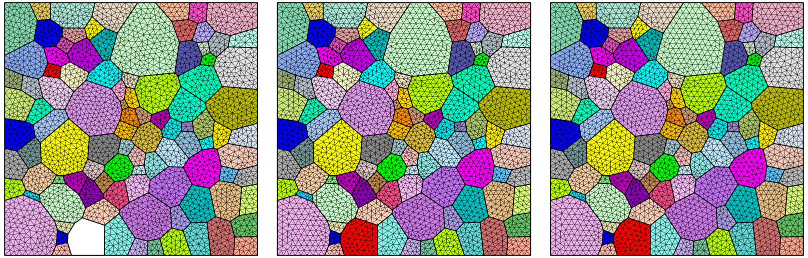

Mesher 1 (Delaunay), Mesher 2 (Frontal), Multimeshing (60% mesher 1, 40% mesher 2)

Remeshing: $\varepsilon = 30\text{–}40\% \rightarrow \varepsilon > 100\%$

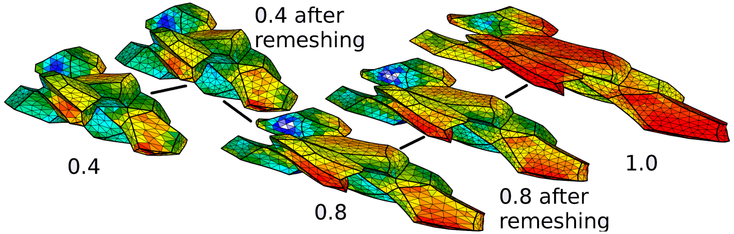

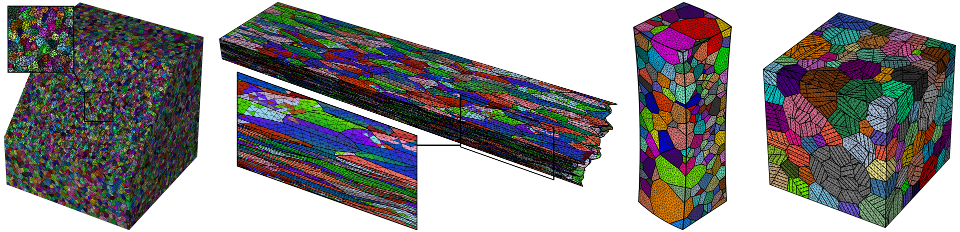

Principle

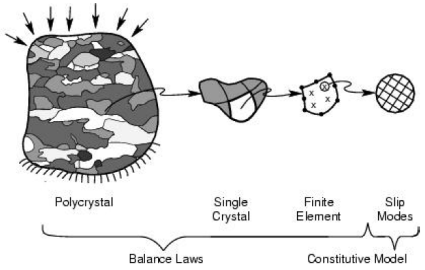

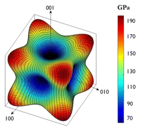

Crystal elasticity

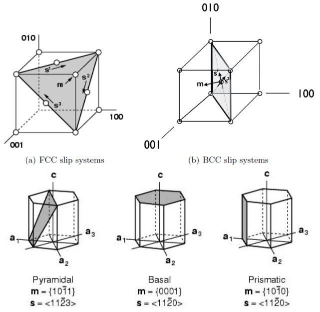

Anisotropic plasticity

Specifics

- Elasto-viscoplastic behavior

$$\dot{\gamma}^{\alpha} = \dot{\gamma}_0 \left(\frac{|\tau^{\alpha}|}{g^{\alpha}} \right)^{1/m} \text{sgn}(\tau^{\alpha})$$

  + Different hardening models (isotropic, anisotropic, precipitation-based, cyclic, etc.)
- Multiphase (cubic, hexagonal, tetragonal)
- General or RVE-type loadings
- Nonlinear kinematics for large strains and large rotations
- State variable evolution for lattice orientation and slip strengths
- Standard and advanced outputs

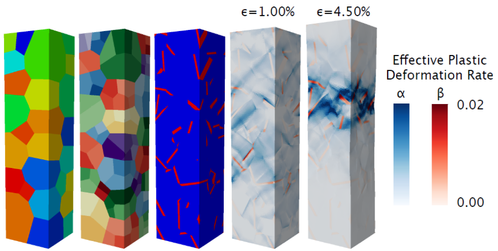

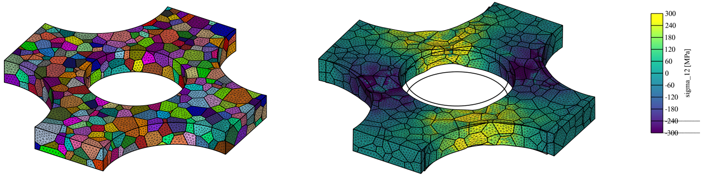

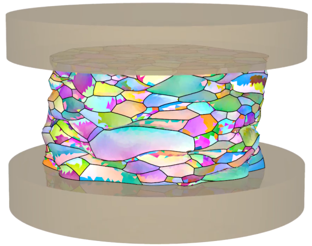

Can simulate deformation of polycrystals with 1000+ grains discretized 10^6 nodes/elements to small or large plastic strain routinely

Outline

The Neper/FEPX Framework

Intra-grain Orientation Distributions in Deformed Aluminium (Acta Materialia, 2024)

Experiment

(Renversade and Quey, 2024)

Sample and Analysis at ESRF / ID11

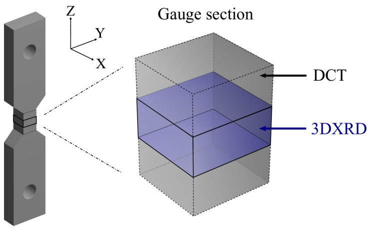

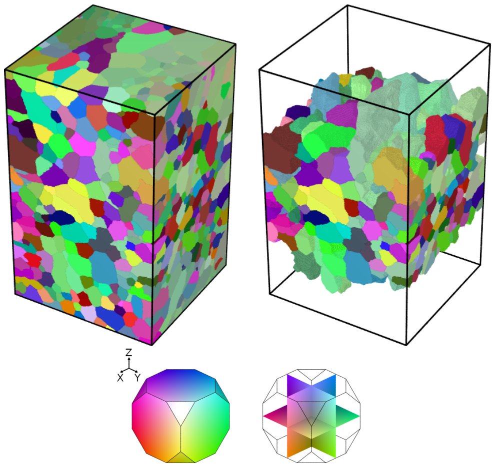

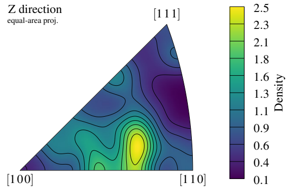

Initial texture

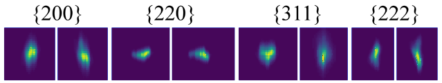

Example spots of a grain at $\varepsilon = 2\%$

- Aluminium alloy (Al0.3Mn), $\bar{d} = 200$ µm
- Uniaxial tension to $\varepsilon = 1.0, 1.5, 2.0, 2.5$ and 4.5%
- DCT at initial state, $\sim$2000 grains

  $\leadsto$ Initial microstructure
- 3DXRD at deformed states, $\sim$700 grains

  $\leadsto$ Spot shapes (azimuthal projection)

Acknowledgements to W. Ludwig (DCT), J. Wright and A. Borbély (3DXRD)

Reduced ODF

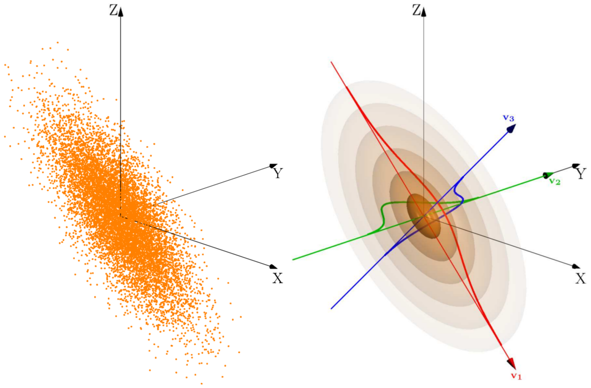

$$P(\mathbf{w}) = \prod_{i=1}^{3} \frac{1}{\sqrt{2\,\pi\,\theta_i^{\,2}}} \exp\left(-\frac{(\mathbf{w}\cdot\mathbf{v}_i)^2}{2\,\theta_i^{\,2}}\right)$$

Forward Modelling

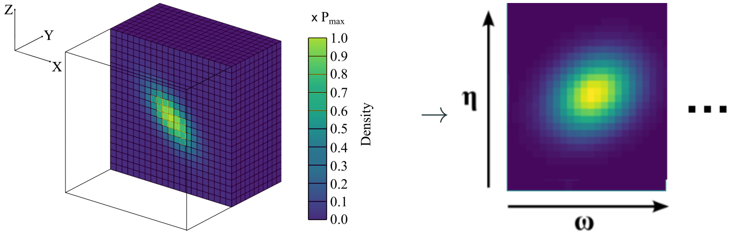

$$r = \frac{\sum_{i,j}\left(I^{ij}_{\text{exp}} - I_{\text{exp}}\right)\left(I^{ij}_{\text{gen}} - I_{\text{gen}}\right)}{\sqrt{\sum_{i,j}\left(I^{ij}_{\text{exp}} - I_{\text{exp}}\right)^2}\sqrt{\sum_{i,j}\left(I^{ij}_{\text{gen}} - I_{\text{gen}}\right)^2}},$$

$$R = \frac{1}{N}\sum_{k=1}^{N} r_k$$

see also (Hansen et al, 2009)

Spots (Azimuthal Projection)

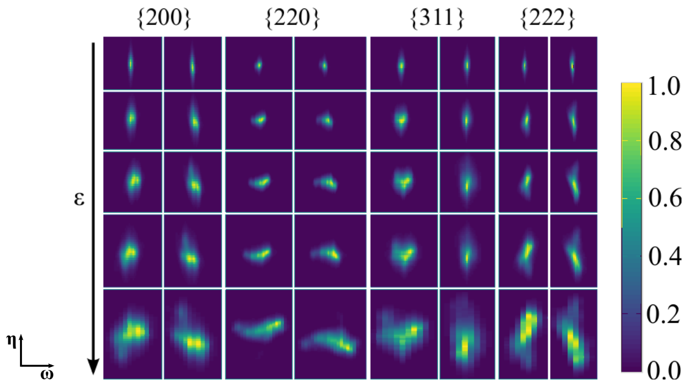

Experiment

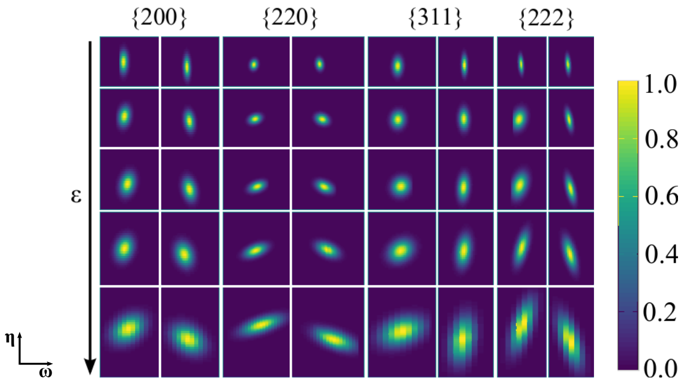

Forward Modelling

End Result = Orientation Distribution

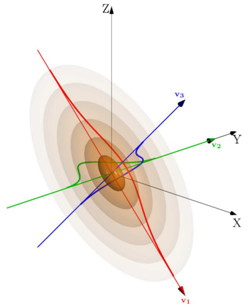

tri-variate normal distribution

$$\mathbf{v}_1 = \begin{bmatrix} 0.96 \\ 0.06 \\ -0.26 \end{bmatrix} \quad \mathbf{v}_2 = \begin{bmatrix} 0.03 \\ 0.94 \\ -0.34 \end{bmatrix} \quad \mathbf{v}_3 = \begin{bmatrix} 0.27 \\ 0.33 \\ -0.90 \end{bmatrix}$$

$$\theta_1 = 0.56^\circ \qquad \theta_2 = 0.25^\circ \qquad \theta_3 = 0.15^\circ$$

Metrics

- Angular extent (“GOS”):

$$\bar{\theta} = \sqrt{2/\pi}\ (\theta_1{}^p + \theta_2{}^p + \theta_3{}^p)^{\frac{1}{p}}\ ,\ p = 1.58$$

- Anisotropy factor: $\theta_a = \theta_1 / \sqrt[3]{\theta_1\,\theta_2\,\theta_3}\ (\geq 1)$
- Preferential disorientation axis: $\mathbf{v_1}$

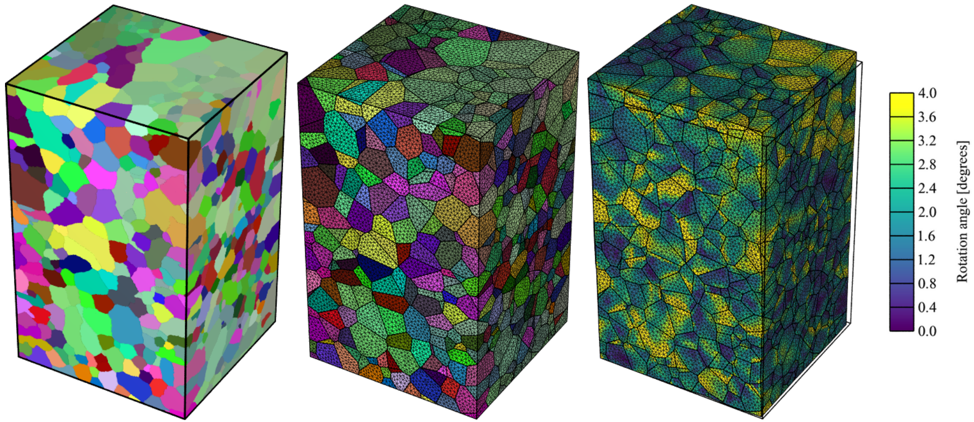

Crystal Behaviour

- $\{111\}\,\langle 110\rangle$ systems
- $\dot{\gamma}^\alpha = \dot{\gamma}_0 \left|\frac{\tau^\alpha}{g^\alpha}\right|^{\frac{1}{m}} \operatorname{sgn}(\tau^\alpha)$

  with $\dot{g}^\alpha = h_0 \left(\frac{g_s - g^\alpha}{g_s - g_0}\right)^{n'} \dot{\gamma}$

  and $\dot{\gamma} = \sum_\alpha |\dot{\gamma}^\alpha|$

  $\dot{\gamma}_0 = 1$, $m = 0.03$, $h_0 = 47$ MPa, $n' = 2.6$, $g_0 = 6$ MPa, $g_s = 455$ MPa

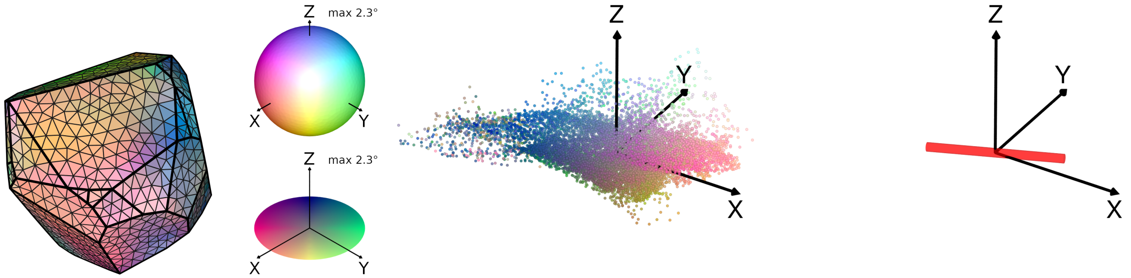

Results

(Glez and Driver, 2001) (Barton and Dawson, 2001)

$$\mathbf{S} = \frac{1}{N}\sum_\alpha (\mathbf{w}^\alpha \otimes \mathbf{w}^\alpha)$$

$$\mathbf{S} = \begin{pmatrix} \lambda_1 & 0 & 0 \\ 0 & \lambda_2 & 0 \\ 0 & 0 & \lambda_3 \end{pmatrix}$$

in $(\boldsymbol{v}_1, \boldsymbol{v}_2, \boldsymbol{v}_3)$ with $\lambda_1 \geq \lambda_2 \geq \lambda_3$

$\rightarrow \overline{\theta}$, θ_a and $\boldsymbol{v}_1$

Angular Extent ($\bar{\theta}$)

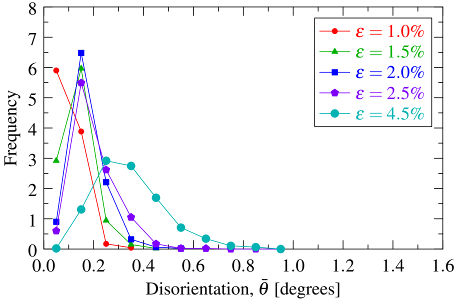

Experiment

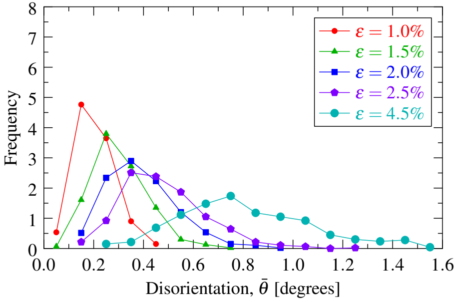

Simulation

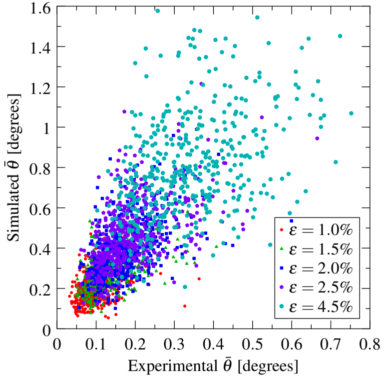

Grain-by-grain comparison

Anisotropy (θ_a)

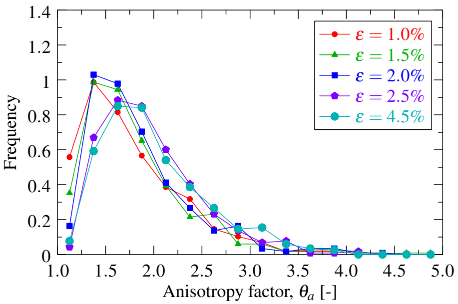

Experiment

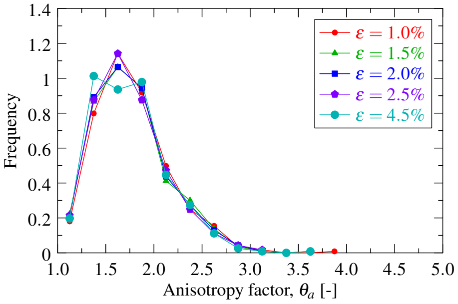

Simulation

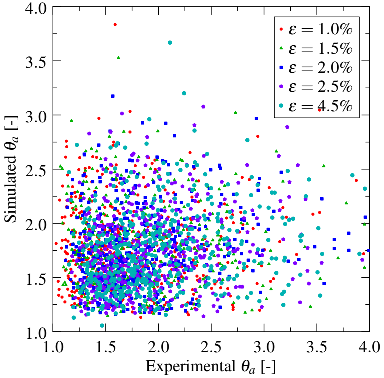

Grain-by-grain comparison

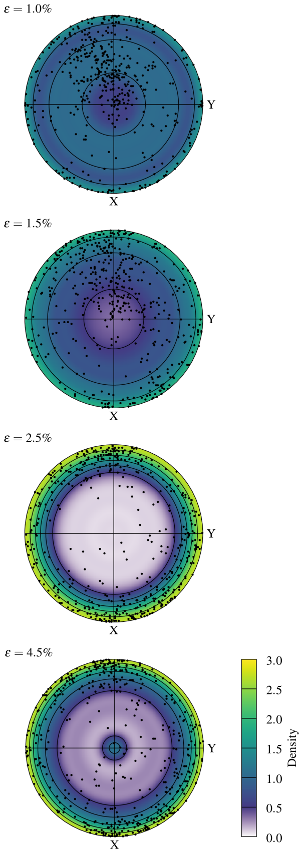

Experiment

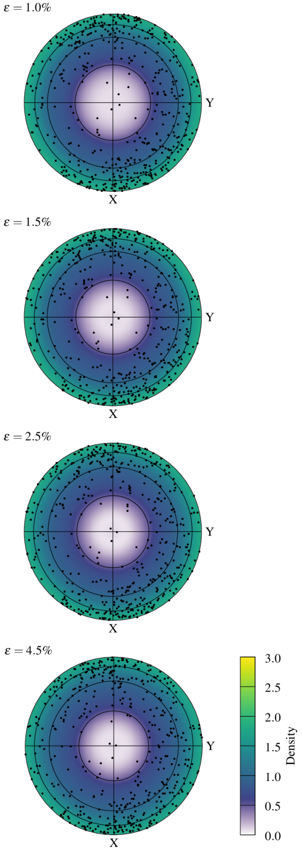

Simulation

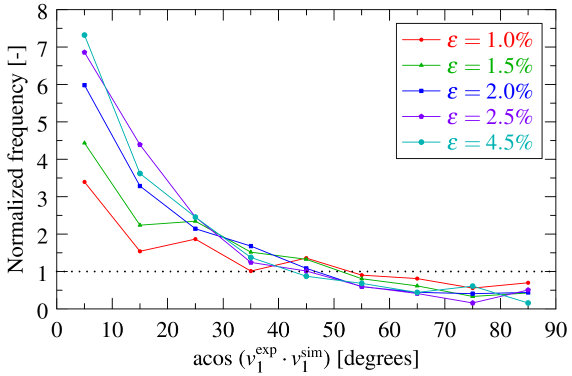

Grain-by-grain comparison

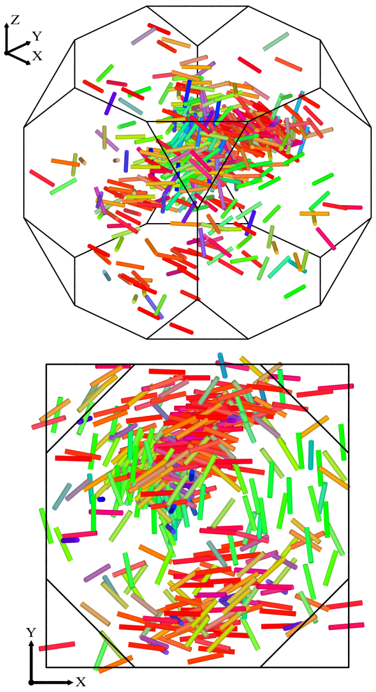

Experiment

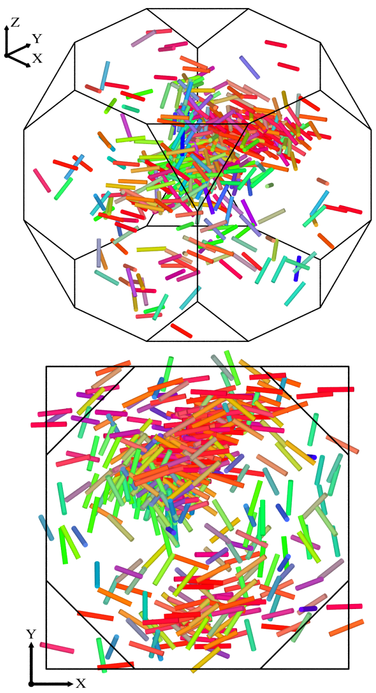

Simulation

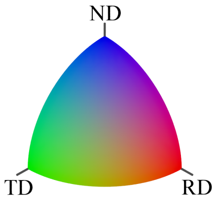

Summary of the Results

Angular extent ($\bar{\theta}$):	regular increase, simulation goes faster	good correlation
Anisotropy factor (θ_a):	similar, self-similar distributions	no correlation
Preferential disorientation axis ($\boldsymbol{v}_1$):	similar RD–TD distribution	good correlation

$\rightsquigarrow$ First-order agreement between experiment and simulation (cross-validation)

To Go Further

- **Option #1: Improve the agreement between experiment and simulation**
  - Experiment: microstructure reconstruction, reduced ODF reconstruction, ...
  - Simulation: microstructure meshing, material model (slip law, slip parameters, interaction matrix, ...) ...

- **Option #2: Learn from the current level of agreement (especially on $\boldsymbol{v}_1$)**

  Simulation particularly useful ($\boldsymbol{v}_1$ and $\boldsymbol{\sigma}$, $\dot{\gamma}^\alpha$, τ^α, etc.)
  - How does the preferential disorientation axis ($\boldsymbol{v}_1$) relate to deformation (slip)?
  - What controls the preferential disorientation axis ($\boldsymbol{v}_1$)?

Summary of the Results

Angular extent ($\bar{\theta}$):	regular increase, simulation goes faster	good correlation
Anisotropy factor (θ_a):	similar, self-similar distributions	no correlation
Preferential disorientation axis ($\mathbf{v}_1$):	similar RD–TD distribution	good correlation

$\rightsquigarrow$ First-order agreement between experiment and simulation (cross-validation)

To Go Further

- **Option #1: Improve the agreement between experiment and simulation**
  - Experiment: microstructure reconstruction, reduced ODF reconstruction, ...
  - Simulation: microstructure meshing, material model (slip law, slip parameters, interaction matrix, ...) ...
- **Option #2: Learn from the current level of agreement (especially on v_1)**

  Simulation particularly useful ($\mathbf{v}_1$ and $\boldsymbol{\sigma}$, $\dot{\gamma}^\alpha$, τ^α, etc.)
  - How does the preferential disorientation axis ($\mathbf{v}_1$) relate to deformation (slip)?
  - What controls the preferential disorientation axis ($\mathbf{v}_1$)?

$$F = V^* R^* F^p \qquad V^* = I + \varepsilon^e \qquad \tau = \mathbb{C} : \varepsilon^e \qquad \tau = \det(I + \varepsilon^e)\, \sigma$$

$$\hat{L}^p = \dot{\hat{F}}^p \hat{F}^{p\,-1} \qquad \hat{L}^p = \hat{D}^p + \hat{W}^p \qquad \hat{D}^p = \sum_\alpha \dot{\gamma}^\alpha \hat{P}^\alpha \qquad \hat{W}^p = \dot{R}^* R^{*T} + \sum_\alpha \dot{\gamma}^\alpha \hat{Q}^\alpha$$

$$\dot{\gamma}^\alpha = \dot{\gamma}_0 \left| \frac{\tau^\alpha}{g^\alpha} \right|^{\frac{1}{m}} \operatorname{sgn}(\tau^\alpha) \qquad \tau^\alpha = \hat{P}^\alpha : \tau \qquad \dot{g}^\alpha = h_0 \left(\frac{g_s - g^\alpha}{g_s - g_0} \right) \dot{\gamma}, \quad \text{where } \dot{\gamma} = \sum_\alpha |\dot{\gamma}^\alpha|$$

$$\varepsilon^e = 0, \quad \hat{W}^p = 0, \quad R^* = I$$

$$\frac{\partial \dot{\boldsymbol{r}}^*}{\partial \boldsymbol{\sigma}_V} = -\sum_\alpha \frac{\partial \dot{\gamma}^\alpha}{\partial \tau^\alpha} \left(\boldsymbol{t}^\alpha \otimes \boldsymbol{p}^\alpha \right) \quad \text{with } \frac{\partial \dot{\gamma}^\alpha}{\partial \tau^\alpha} = \frac{\dot{\gamma}_0}{m\, g^\alpha} \left| \frac{\tau^\alpha}{g^\alpha} \right|^{\frac{1}{m}-1} \tag{1}$$

$$\frac{\partial \dot{r}^*}{\partial \sigma_V} = U S V^T \tag{2}$$

$\frac{\partial \dot{\boldsymbol{r}}^*}{\partial \boldsymbol{\sigma}_V}$ can be *(i)* evaluated for different (nominal) stresses and *(ii)* associated to different stress distributions

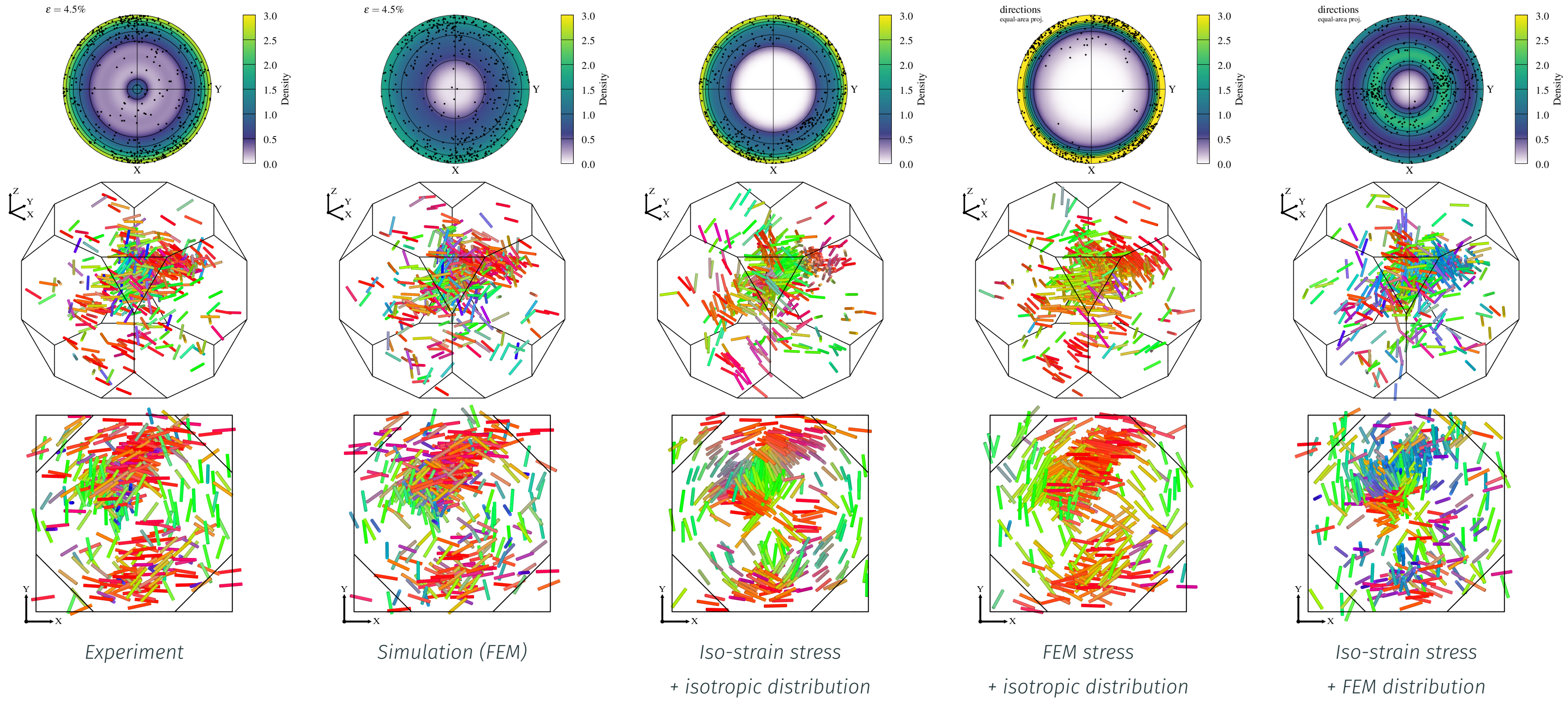

Preferential disorientation axis sensitive to average grain stress, not stress distribution

Conclusions

Neper/FEPX

- Convergence between two "established" codes
- Complete workflow, especially for experiment-simulation comparisons (`.tesr`, `.sim`, etc.)

Application to Intra-Grain Orientation Distributions

- Various approximations made along the way, in both experiment and simulation…
- 1st-order agreement between experiment and simulation (validation)
- Simulation results (stresses, slip rates, strengths, etc.) used to go further
- Preferential disorientation axis sensitive to stress, not so much to stress distribution

Example of how experiment and simulation can be used

to improve our understanding of material deformation